

MODELLING TURBULENT HEAT TRANSPORT IN PLANAR HOT JETS WITH DIFFERENT TURBULENT CLOSURES

S. Rochhausen, C. Morsbach and E. Kügeler

Institute of Propulsion Technology
Department of Numerical Methods
German Aerospace Center (DLR)
Linder Höhe, 51147 Cologne, Germany
stefan.rochhausen@dlr.de

INTRODUCTION

Modern high pressure turbines are cooled by ejecting coolant flow from holes, which protects the material from overheating. In order to evaluate novel cooling designs there is a demand for quick and robust CFD tools, that deliver accurate predictions of cooling flow systems. From an aerodynamic point of view it is crucial to have a good representation of turbulent mixing of hot and cold flow with different velocities.

Performing LES simulations in turbine cooling problems is currently too expensive in terms of computational power. State-of-the-art in industrial turbine design is to use two-equation eddy viscosity turbulence models. It would be desirable to obtain high quality predictions for cooling configurations from this numerical setup. However, previous investigations by Beuermann *et al.* (2012) have shown that film cooling efficiency is predicted significantly higher compared to experiments. It is assumed that turbulent mixing is underpredicted.

The planar hot jet flow is the simplest representation of a turbulent shear flow with a high relevance for film cooling applications. It is known from this type of flow that there is a difference in the lateral extent of velocity and scalar (temperature) fields. The temperature field of a hot turbulent two-dimensional jet, is approximately 30% wider than its velocity wake (cf. Schlichting & Gersten (2006)). This observation is poorly represented with current industrial RANS simulations applying eddy viscosity models and the Reynolds analogy as turbulent heat flux closure. Typically a constant turbulent Prandtl number of $Pr_T = 0.9$ is used, which gives good predictions in attached boundary layers. For free shear layers, such as the turbulent jet, a turbulent Prandtl number of 0.5 is proposed in literature (Schlichting & Gersten (2006)). A cooled turbine flow field contains numerous shear and boundary layers. To improve the solution accuracy more sophisticated models for turbulent heat flux must deliver good predictions in both types of flow.

In this work the performance of different combinations of models for turbulent momentum and heat flux are compared with respect to their ability to predict the temperature and velocity field of a planar turbulent hot jet and heat transfer coefficient of a flat plate boundary layer. The spectrum of closure levels ranges from two-equation linear models to anisotropy resolving differential Reynolds stress models.

NUMERICAL METHOD AND TURBULENCE MODELLING

The flow solver applied in this work is TRACE - the DLR standard solver for turbomachine flow simulations. The solver is applied in industrial turbomachine design as well as in research projects. It solves the compressible Favre-averaged Navier Stokes equations in a finite volume framework on multiple block meshes. Further details on the flow solver can be found in Becker *et al.* (2010). Various turbulence models are available in TRACE. The models used in this investigation will be discussed in the following.

As a representative for the isotropic linear eddy viscosity model class, the SST- $k\omega$ -model by Menter (1994) has been chosen. This model has been combined with simple gradient diffusion (Reynolds analogy) $Pr_T = 0.9$ (equation 1). Due to its high numerical stability, this modelling combination is the current standard in industrial calculations. The SST- $k\omega$ -model can also be combined with an isotropic two equation eddy conductivity transport model (ECTM): The $k_\theta\omega_\theta$ -model (equation 2) for the turbulent heat flux. The $k_\theta\omega_\theta$ -model is a reformulation by Rochhausen (2012) of the $k_\theta\varepsilon_\theta$ -model of Nagano & Kim (1988) that solves the transport equations for temperature variance k_θ and its dissipation rate ε_θ . Further details on the transport equations and the model constants can be found in Rochhausen (2012).

Reynolds Analogy (PRT)

$$-\overline{\rho u_j'' h''} = \rho c_p \left[\frac{k}{\omega} \frac{1}{Pr_T} \right] \frac{\partial T}{\partial x_j} \quad (1)$$

$k_\theta\omega_\theta$ (ECTM)

$$-\overline{\rho u_j'' h''} = \rho c_p \left[C_\theta \frac{k}{\sqrt{\omega \omega_\theta}} \right] \frac{\partial T}{\partial x_j} \quad (2)$$

Two modern anisotropy resolving turbulence models, a differential and an explicit algebraic Reynolds stress model, are tested in this investigation. The Reynolds stress transport model class is represented by the SSG/LRR- ω model by Eisfeld (2010). Compared to other Reynolds stress transport models, the SSG/LRR- ω -model is known to be relatively stable and has been successfully applied in complex flow. Differential Reynolds stress models in combination with higher order closures for the turbulent heat

	Reynolds analogy	Eddy conductivity models	Algebraic heat flux models
Eddy viscosity modelling	SST PRT	SST ECTM	
Explicit algebraic Reynolds stress modelling	EARSM PRT		EARSM DH EARSM YSC
Differential Reynolds stress modelling	SSGLRR PRT		SSGLRR DH SSGLRR YSC

Table 1. Model combinations and abbreviations

flux might be a promising alternative that is able to represent the physical processes in a turbulent flow, but they are not yet applied in industrial design due to stability issues. The explicit algebraic Reynolds stress model class is represented by the EARSM- $k\omega$ -model of Hellsten (2005). This model is a compromise between eddy-viscosity and differential Reynolds stress modelling: It is based on the Boussinesq-assumption and adds extra anisotropy to the Reynolds stresses. Thus it combines a higher numerical stability with a better representation of the physical processes.

For the turbulent heat flux two anisotropy resolving algebraic heat flux models are applied: A simple model - the Daly & Harlow (1970) approach (equation 3) - which is often referred to as the generalized gradient diffusion approach. Here the thermal diffusivity depends on Reynolds stresses - the model allows the thermal diffusivity to be anisotropic. Additionally a more complex approach by Younis *et al.* (2005) (equation 4) will be used. This model has been derived by tensor representation theory. In addition to the Daly & Harlow model it takes into account the dependence of mean deformation rate and thermal diffusivity and the model coefficient C_{r1}^* is modified in the near wall region via damping function (Uddin *et al.* (2009)). For the Daly & Harlow approach the constant $C = 0.3$ has been used; for the modelling constants of the Younis-model see Younis *et al.* (2005). All model combinations that have been tested can be found in table 1.

Daly & Harlow (DH)

$$-\overline{\rho u_j'' h''} = \rho c_p \left[C \frac{\overline{u_i' u_j'}}{\omega} \right] \frac{\partial T}{\partial x_j} \quad (3)$$

Younis *et al.* (YSC)

$$-\overline{\rho u_i'' h''} = \rho c_p \left[C_{r1}^* \frac{k}{\omega} \right] \frac{\partial T}{\partial x_i} + \rho c_p \left[C_{r2} \frac{\overline{u_i' u_j'}}{\omega} + C_{r3} \frac{k}{\omega^2} \frac{\partial U_i}{\partial x_j} - C_{r4} \frac{P_{ij}}{\omega^2} \right] \frac{\partial T}{\partial x_j} \quad (4)$$

TESTCASES

The computational domain of the turbulent jet consists of 160 (lateral) \times 100 (streamwise) cells. At inflow and outflow boundaries constant properties have been set. All other boundaries have been set to symmetric. The full mesh extends 121 jet diameters in lateral direction. The size in flow

direction is 200 jet diameters. The Reynolds number based on jet diameter is about 30,000, the Mach number is 0.24. The temperature ratio is $\frac{T_{jet}}{T_\infty} = \frac{450K}{300K} = 1.5$. A schematic overview over the jet and the most important flow quantities is given in Figure 1.

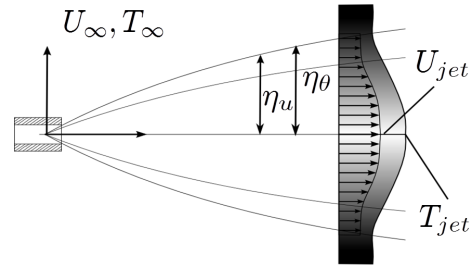


Figure 1. Overview of the jet test case.

The flat plate test case has a Reynolds number based on plate length of 5.0 Mio and a Mach number of about 0.1. The plate is heated with constant temperature boundary condition of $\Delta T = T_w - T_\infty = 20K$. A low Reynolds mesh resolution is used with an y^+ -value of approximately 1 and a cell growth rate of 20% orthogonal to the wall. At inflow and outflow boundaries constant properties have been set. All other boundaries have been set to symmetric. The full mesh extends 60 cells in lateral direction and 200 cells in streamwise direction. A schematic overview over the flat plate and the most important flow quantities is given in Figure 2.

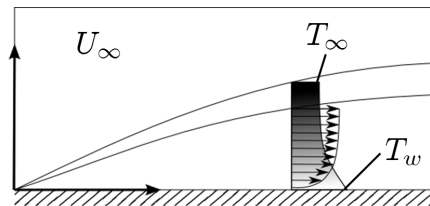


Figure 2. Overview of the flat plate test case.

RESULTS

Turbulent Jet

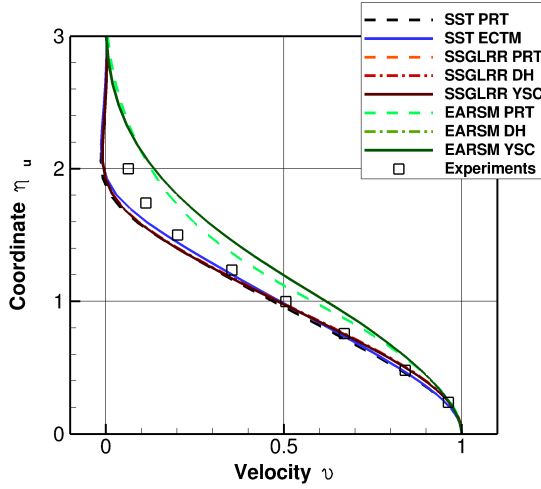


Figure 3. Lateral velocity profiles.

Figure 3 shows streamwise velocity profiles $v = \frac{u}{u_{max}}$ versus the lateral coordinate $\eta_u = \frac{y}{y_{0.5u}}$ that has been normalized with a reference jet velocity half-width $y_{0.5u} = A(x - x_0)$. In those simulations that have been made with SST- $k\omega$ and SSG/LRR- ω the velocity distributions can be predicted in good agreement with the measurements by Shih *et al.* (1990). The turbulent heat flux treatment has no significant effect on the velocity distribution. The simulations that have been performed with explicit algebraic Reynolds stress modelling show a greater lateral extent of the velocity field.

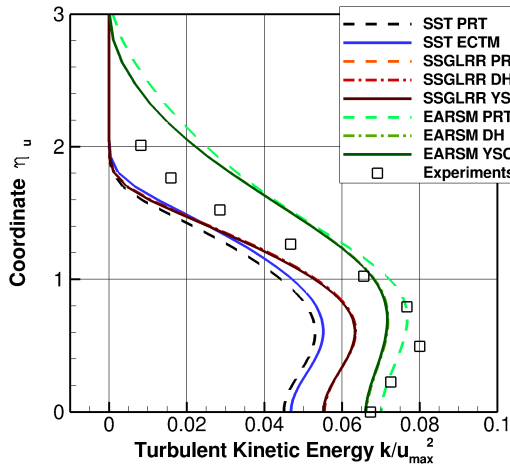


Figure 4. Lateral turbulent kinetic energy profiles.

The explanation for the differences in the lateral extent

of the velocity fields can be found in the turbulent kinetic energy distribution. Figure 4 shows lateral profiles of turbulent kinetic energy $\frac{k}{u_{max}^2}$ versus the jet velocity half-width η_u . The simulations SST- $k\omega$ and SSG/LRR- ω have similar turbulent kinetic energy profiles with a smaller lateral extent and a lower peak value than observed in the experiments. The EARS M-simulation in contrast overpredicts the lateral extent of the kinetic energy.

In analogy to the velocity profiles, figures 5, 6 and 7 show temperature profiles $\theta = \frac{T - T_\infty}{T_{max} - T_\infty}$ versus the lateral coordinate $\eta_\theta = \frac{y}{y_{0.5\theta}}$ that has been normalized with the reference jet temperature half-width with $y_{0.5\theta} = B(x - x_0)$. The constants A and B describe the measured linear growth of the lateral extent of a planar jet in streamwise direction (Schlichting & Gersten (2006)). A and B differ by about $\frac{B}{A} = 1.27$. Thus the half-width of the temperature field is 27% larger than the velocity half-width. The lateral coordinates for temperature and velocity half-width are shown in figure 1.

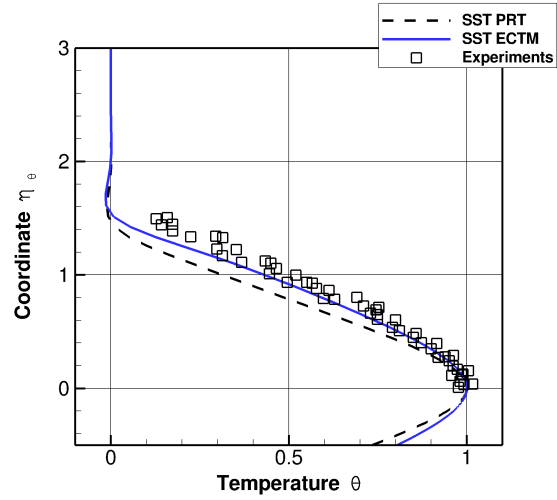


Figure 5. Lateral temperature profiles, SST-models.

Figures 5-7 show the same trend: those calculations made with constant Prandtl number $Pr_T = 0.9$ (SST-PRT, EARS M-PRT, SSGLRR-PRT) show a smaller lateral extent in temperature compared to calculations made with higher order heat flux models.

At the position $\theta = 0.5$ the different lateral extent of measurements and simulation can be quantified. The combination SST-PRT underpredicts the lateral extent by about 20%. The eddy conductivity model (SST-ECTM) shows a better prediction with less than 10% deviation from the experimental data.

The application of the differential Reynolds stress model with constant Prandtl number $Pr_T = 0.9$ (SSGLRR-PRT) leads to a temperature field similar to the one calculated with the eddy viscosity based combination (SST-PRT). In the Reynolds stress calculation the use of algebraic heat flux models (SSGLRR-DH & SSGLRR-YSC) show a significantly larger lateral extent of the temperature field. The Daly & Harlow - model gives the best agreement with 7% deviation from the experimental data. The Younis model predicts a deviation of roughly 10%.

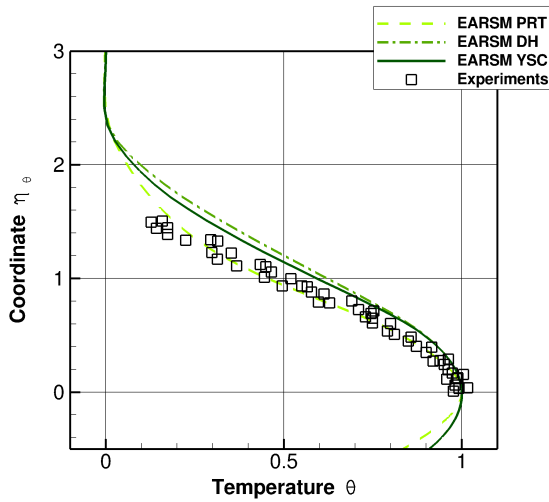


Figure 6. Lateral temperature profiles, EARSM-models.

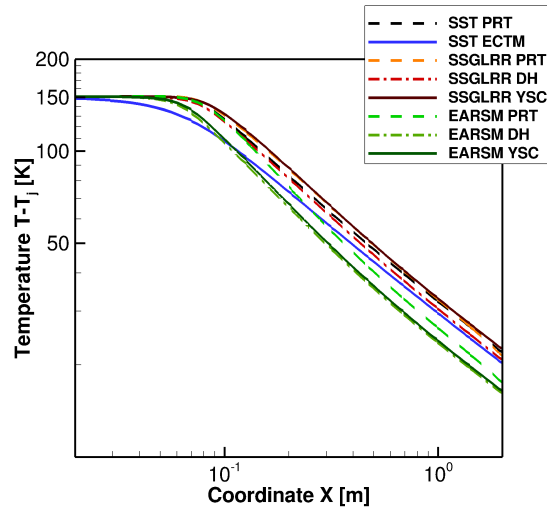


Figure 8. Streamwise temperature distribution.

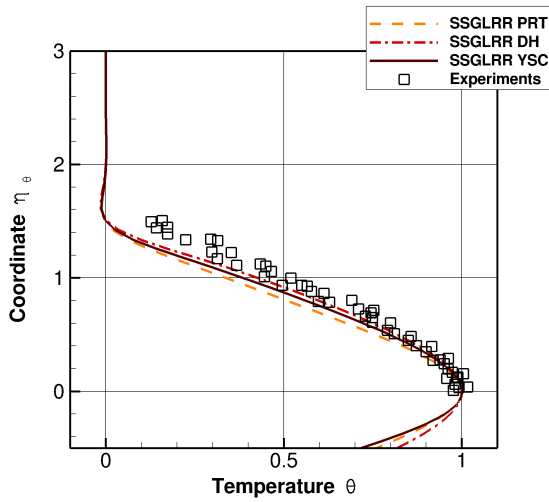


Figure 7. Lateral temperature profiles, SSGLRR-models..

The temperature field calculated with the Hellsten EARSM is generally wider than those calculated with SST or SSGLRR. This can be explained with the different velocity field. However, as in the SSGLRR-calculations, the application of algebraic heat flux models (EARSM-DH & EARSM-YSC) leads to a larger lateral extent of the temperature field. Again, the Daly & Harlow model shows a slightly larger lateral temperature field than the field calculated with the Younis model.

In figure 8 the maximum jet centerline temperature is plotted versus the x-Coordinate. The greater lateral extent of the temperature fields, predicted by the higher order heat flux models, leads to a faster mixing of the jet. At a given x-Position, the highest peak temperature in the wake center correlates with the smallest lateral extent of the temperature wake.

Flat Plate Boundary Layer

In the figures 9 and 10 the flat plate testcase is shown. Figure 9 shows the Stanton number distribution for all

model combinations compared to the correlation by Kays & Crawford (1980). All the numerical results are located within the $\pm 10\%$ -error band relative to the correlation. The curves can be subdivided into two groups, all simulations using algebraic heat flux modelling (EARSM-DH/-YSC & SSGLRR-DH/-YSC) show slightly higher Stanton numbers compared to the correlation. All other simulations show slightly lower Stanton numbers.

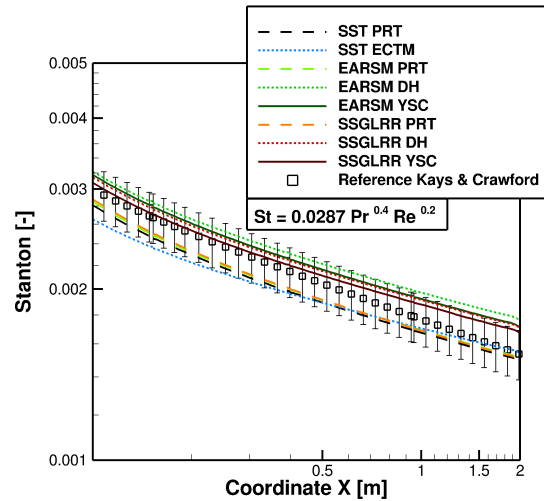


Figure 9. Stanton numbers.

Figure 10 shows the non-dimensional temperature t^+ versus the non-dimensional wall distance y^+ at $x = 1.5m$ compared with law of the wall for thermal boundary layers by Kays & Crawford (1980). Here again, the curves can be subdivided into two groups. In the turbulent region the algebraic heat flux model group has the same gradient as the correlation. The other group shows a steeper gradient, but the absolute level is in good agreement with the correlation.

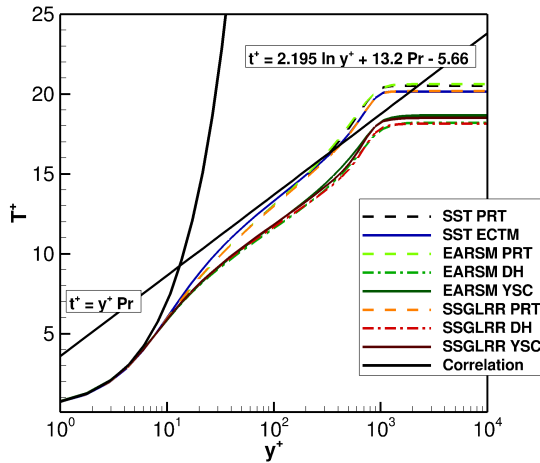


Figure 10. Non-dimensional temperature t^+ .

CONCLUSION

Eight different combinations of models for turbulent momentum and heat flux have been compared numerically with respect to their ability to predict the mixing of hot and cold flow in a planar hot jet and the heat transfer rate of a heated flat plate boundary layer.

For the heated jet it has been shown that the current standard approach for the turbulent heat flux - the Reynolds analogy - predicts a narrow temperature field. The lateral extent of the temperature field can be increased by using more sophisticated models for the turbulent heat flux. A linear eddy conductivity model and two algebraic heat flux models have been presented, that show a better prediction of the temperature field of the turbulent jet.

All model combinations have been tested in the turbulent flat plate boundary layer. The current standard model - a constant Prandtl number $Pr_T = 0.9$ - is known for good heat transfer rate predictions for attached boundary layers. Compared to the correlations the explicit algebraic heat flux models increase the heat transfer rates by less than 10 percent. Generally the deviations from the flat plate correlations are small. Thus it can be concluded that the higher order models for the turbulent heat flux, that have been presented in this investigation, do not alter the flat plate heat transfer predictions relative to a constant Prandtl number $Pr_T = 0.9$ modelling.

In this work the combination of Reynolds stress modelling combined with explicit algebraic heat flux models is the most accurate way of predicting cooling flows. This model combination increases the accuracy in the investigated hot jet and predicts the flat plate boundary layer according to the correlations. The turbulent heat flux is represented by a vector and the energy transport can be considered in each flow direction. More detailed information about this will be presented in future studies. With regard to numerical robustness the two-equation eddy conductivity model might be an interesting choice as well, at least for

industrial applications. Integral values such as the lateral temperature extent of the jet can be predicted with a better accuracy. Depending on the complexity of the problem considered all closure levels have their merits. Further studies on more complex geometries such as a cooled turbine and detailed information on the turbulent heat flux vector are

needed to evaluate model accuracy.

REFERENCES

- Becker, Kai, Heitkamp, Kathrin & Kügeler, Edmund 2010 Recent progress in a hybrid-grid CFD solver for turbomachinery flows. In *Proceedings Fifth European Conference on Computational Fluid Dynamics ECCOMAS CFD 2010*.
- Beuermann, Annette, Pabs, Andreas & Rochhausen, Stefan 2012 Numerical investigation of heat transfer and cooling effectiveness within a lpt-vane cascade and its comparison to experimental results. In *ASME Turbo Expo 2012: Turbine Technical Conference and Exposition. American Society of Mechanical Engineers*.
- Daly, Bart J. & Harlow, Francis H. 1970 Transport equations in turbulence. *Physics of Fluids* **13**, 2634–2649.
- Eisfeld, Bernhard 2010 Reynolds stress modelling for complex aerodynamic flows. In *V European Conference on Computational Fluid Dynamics ECCOMAS CFD 2010*. Lisbon, Portugal.
- Hellsten, A. K. 2005 New advanced kw turbulence model for high-lift aerodynamics. *AIAA journal* **43**, 1857–1869.
- Kays, W. M. & Crawford, M. E. 1980 *Convective Heat and Mass Transfer*, 2nd edn. McGraw-Hill.
- Menter, Florian R. 1994 Two-equation eddy-viscosity turbulence models for engineering applications. *AIAA journal* **32**, 1598–1605.
- Nagano, Y. & Kim, C. 1988 A two-equation model for heat transport in wall turbulent shear flows. *Journal of heat transfer* **110**, 583–589.
- Rochhausen, S. 2012 Reformulation of a two-equation model for the turbulent heat transfer. In *7th International Symposium on Turbulence, Heat and Mass Transfer*. Palermo, Sicily, Italy.
- Schlichting, H. & Gersten, K. 2006 *Grenzschichttheorie*, 10th edn. Springer-Verlag.
- Shih, T-H., Lumley, J. L. & Chen, J-Y. 1990 Second-order modeling of a passive scalar in a turbulent shear flow. *AIAA journal* **28**, 610–617.
- Uddin, Naseem, Neumann, Sven Olaf, Weigand, Bernhard & Younis, Bassam A. 2009 Large-eddy simulations and heat-flux modeling in a turbulent impinging jet. *Numerical Heat transfer, Part A: Applications* **55.10**, 906–930.
- Younis, Bassam A., Speziale, Charles G. & Clark, Timothy T. 2005 A rational model for the turbulent scalar fluxes. In *Proceedings of the Royal Society A: Mathematical, Physical and Engineering Science*, , vol. 461, pp. 575–594.